MATCH
Communications in Mathematical and in Computer Chemistry

MATCH Commun. Math. Comput. Chem. **96** (2026) 353–382
ISSN: 0340–6253
doi: 10.46793/match.96-1.10525

On the Distribution of Topological and Spectral Indices on Random Graphs

Claudia Teresa Martínez-Martínez[a,b,*], **Rocío Aguilar-Sánchez**[c], **José Antonio Méndez-Bermúdez**[d]

[a] *Facultad de Matemáticas, Universidad Autónoma de Guerrero, Acapulco de Juárez 39650, Mexico,*

[b] *Facultad de Ciencias, Universidad Autónoma Benito Juárez de Oaxaca, Oaxaca de Juárez 68120, Mexico*

[c] *Facultad de Ciencias Químicas, Benemérita Universidad Autónoma de Puebla, Puebla 72570, Mexico*

[d] *Instituto de Física, Benemérita Universidad Autónoma de Puebla, Puebla 72570, Mexico*

cl4ud7@gmail.com, ras747698@gmail.com, jmendezb@ifuap.buap.mx

(Received May 6, 2025)

Abstract

We perform a detailed statistical study of the distribution of topological and spectral indices on random graphs $G = (V, E)$ in a wide range of connectivity regimes. First, we consider degree-based topological indices (TIs), and focus on two classes of them: $X_\Sigma(G) = \sum_{uv \in E} f(d_u, d_v)$ and $X_\Pi(G) = \prod_{uv \in E} g(d_u, d_v)$, where uv denotes the edge of G connecting the vertices u and v, d_u is the degree of the vertex u, and $f(x, y)$ and $g(x, y)$ are functions of the vertex degrees. Specifically, we apply $X_\Sigma(G)$ and $X_\Pi(G)$ on Erdös-Rényi graphs and random geometric graphs along the full transition from almost isolated vertices to mostly connected graphs. While

*Corresponding author.

we verify that $P(X_\Sigma(G))$ converges to a standard normal distribution, we show that $P(X_\Pi(G))$ converges to a log-normal distribution. In addition we also analyze Revan-degree-based indices and spectral indices (those defined from the eigenvalues and eigenvectors of the graph adjacency matrix). Indeed, for Revan-degree indices, we obtain results equivalent to those for standard degree-based TIs. Instead, for spectral indices, we report two distinct patterns: the distribution of indices defined only from eigenvalues approaches a normal distribution, while the distribution of those indices involving both eigenvalues and eigenvectors approaches a log-normal distribution.

1 Introduction

In chemical graph theory, graph invariants are widely used to characterize the structural properties of graphs [6,27,30]. These invariants can be classified mainly into two types: Topological indices (TIs) and multiplicative topological indices (MTIs). TIs are typically defined as sums over vertex or edge functions, such as

$$X_{\Sigma,F_V}(G) = \sum_{u\in V(G)} F_V(d_u) \quad \text{or} \quad X_{\Sigma,F_E}(G) = \sum_{uv\in E(G)} F_E(d_u,d_v) \tag{1}$$

while MTIs are defined as products over vertex or edge functions, such as

$$X_{\Pi,F_V}(G) = \prod_{u\in V(G)} F_V(d_u) \quad \text{or} \quad X_{\Pi,F_E}(G) = \prod_{uv\in E(G)} F_E(d_u,d_v)\,. \tag{2}$$

Here uv denotes the edge of the graph $G = (V(G), E(G))$ connecting the vertices u and v, d_u is the degree of the vertex u, and $F_X(x)$ and $F_X(x,y)$ are appropriate chosen functions, see e.g. [13]. While both $X_\Sigma(G)$ and $X_\Pi(G)$ are referred to as topological indices in the literature, to make a distinction between them, here we name $X_\Sigma(G)$ as topological indices (TIs) and $X_\Pi(G)$ as *multiplicative* topological indices (MTIs). Some prominent examples of TIs are the Randić index [26], the Zagreb indices [15], and the Sombor index [14], while among the MTIs we can mention the Narumi-Katayama index [24] and the multiplicative versions of the Zagreb indices [31]. All these indices (to be defined later), among others, will be analyzed below.

More recently, a new class of TIs based on the Revan vertex degree has been introduced, see e.g. [2, 17–20]. The *Revan vertex degree* of the vertex u is defined as

$$r_u = \Delta + \delta - d_u, \tag{3}$$

where Δ and δ are the maximum and minimum degrees among the vertices of the graph G, respectively. Revan-degree indices, defined as

$$RX_\Sigma(G) = \sum_{uv \in E(G)} F(r_u, r_v) \quad \text{or} \quad RX_\Pi(G) = \prod_{uv \in E(G)} F(r_u, r_v) \tag{4}$$

are the Revan analogs of standard TIs and MTIs, respectively. That is, $RX_\Sigma(G)$ is the Revan version of $X_\Sigma(G)$ and $RX_\Pi(G)$ is the Revan version of $X_\Pi(G)$. In this work, we also explore the distributions of Revan-degree indices.

Additionally, spectral indices, defined in terms of the eigenvalues and eigenvectors of the graph adjacency matrix, have gained attention due to their ability to capture global graph properties avoiding the problem of degeneracy, present in standard TIs; see e.g. [28]. Specifically, we compute the so-called Rodríguez-Velázquez indices [4, 28] as well as the graph energy [16, 21] and the subgraph centrality [10] (to be defined later).

The use of topological and spectral indices on random graphs is relatively recent. Moreover, since a given parameter set represents an infinite-size ensemble of random graphs, the computation of a graph invariant on a single graph may be irrelevant. In contrast, the computation of the average value of a graph invariant over a large ensemble of random graphs, all characterized by the same parameter set, may provide useful average information about the full ensemble. This statistical approach, well known in random matrix theory (RMT) studies, has been recently applied to random graphs and networks by means of topological and spectral indices, see e.g. [1–5, 22, 23]. In fact, the average value of some topological indices have been shown to be equivalent to standard RMT measures [3, 4].

While most studies of topological and spectral indices on random graphs have been focused on the average values of the indices, just a few have considered their probability distribution functions numerically [22, 23] and analytically [33, 34]. Specifically, on the one hand, in Refs. [22, 23] the probability distribution functions of the Randić index, the harmonic index, the sum-connectivity index, the modified Zagreb index, and the inverse degree index on Erdös-Rényi graphs were reported. On the other hand, in Refs. [33, 34] the the probability distribution functions of TIs on Erdös-Rényi graphs and of the Randić index on random geometric graphs were studied; see also the related Refs. [32, 35].

Therefore, in this work to go a step forward in the direction addressed by Refs. [22,23,33,34], we conduct a comprehensive statistical (numeirical) analysis of the probability distribution functions (from now on we will call them just distributions) of TIs, MTIs, Revan-degree indices, and spectral indices on two types of random graphs: Erdös-Rényi graphs (ERGs) and random geometric graphs (RGGs).

This paper is organized as follows. In Sec. 2 we introduce the graph models and the parameter settings to be used in the numerical analysis. In Sec. 3 we report the distributions of TIs, MTIs, Revan-degree indices, and spectral indices on ERGs. To avoid text saturation, the results corresponding to RGGs are reported in the Appendix. Finally, our findings are summarized in Sec. 4.

2 Graph models and parameter settings

ERGs [8, 9, 29], $G_{\rm ERG}(n,p)$, are formed by n vertices connected independently with probability $p \in [0,1]$. While RGGs [7, 25], $G_{\rm RGG}(n,r)$, consist of n vertices uniformly and independently distributed on the unit square, where an edge connects two vertices if their Euclidean distance is less or equal than the connection radius $r \in [0, \sqrt{2}]$.

Our study spans the full transition from almost isolated nodes ($p \to 0$ or $r \to 0$) to almost complete graphs ($p \to 1$ or $r \to \sqrt{2}$), providing insights into the behavior of the indices across different connectivity regimes. In order to clearly set the connectivity regime on both random graph models we will use the average number of non isolated vertices $\langle V(G) \rangle$, which can also be regarded as a TI, see e.g. [3].

Since $\langle V(G) \rangle = 0$ for graphs with only isolated nodes and $\langle V(G) \rangle = n$ when all nodes are connected, $\langle V(G) \rangle$ shows a smooth transition from 0 to n by increasing p from 0 to 1 for ERGs or by increasing r from 0 to $\sqrt{2}$ for RGGs. This is indeed shown in Figs. 1(a) and 1(b) where we present $\langle V(G) \rangle$, normalized to the graph size n, for ERGs as a function of p and for RGGs as a function of r, respectively. There, different symbols correspond to different graph sizes.

As well as for other TIs (see e.g. [1, 5, 22, 23]) the average degree $\langle k \rangle$ serves as the scaling parameter of $\langle V(G) \rangle / n$ [3]; meaning that the curve $\langle V(G) \rangle / n$ vs. $\langle k \rangle$ is a universal curve. This is verified in Figs. 1(c) and 1(d) where we plot, respectively, $\langle V(G) \rangle / n$ for ERGs and RGGs as a function of $\langle k \rangle$: I.e., curves for different graph sizes fall one on top of the other. Note that the functional dependence of $\langle k \rangle$ on the graph parameters is significantly different for both graph models; while for ERGs

$$\langle k \rangle = p(n-1), \tag{5}$$

for RGGs it takes the form

$$\langle k \rangle = g(r)(n-1) \tag{6}$$

with [11]

$$g(r) = \begin{cases} r^2\left[\pi - \frac{8}{3}r + \frac{1}{2}r^2\right], & 0 \le r \le 1\,, \\ \frac{1}{3} - 2r^2\left[1 - \arcsin(1/r) + \arccos(1/r)\right] & \\ \qquad + \frac{4}{3}(2r^2+1)\sqrt{r^2-1} - \frac{1}{2}r^4, & 1 \le r \le \sqrt{2}\,. \end{cases} \tag{7}$$

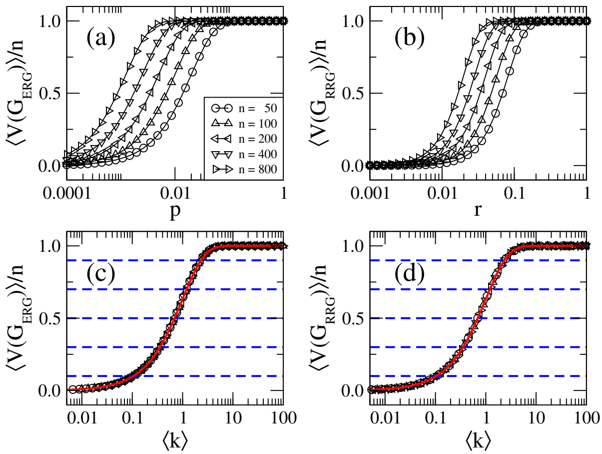

Figure 1. Average number of non isolated vertices $\langle V(G)\rangle$, normalized to the graph size n, for Erdős-Rényi graphs as a function of (a) the probability p and (c) the average degree $\langle k\rangle = p(n-1)$. $\langle V(G)\rangle/n$ for random geometric graphs as a function of (b) the connection radius r and (d) the average degree $\langle k\rangle = g(r)(n-1)$, see Eq. (7). The blue horizontal dashed lines in (c,d) indicate the values of $\langle V(G)\rangle/n$ used to construct the histograms in Figs. 2-12: $\langle V(G)\rangle/n = 0.1$, 0.3, 0.5, 0.7 and 0.9. Each data value was computed by averaging over 10^6 random graphs G.

Then, the curves $\langle V(G)\rangle/n$ vs. $\langle k\rangle$ in Figs. 1(c) and 1(d) allow us to set both graph models in a given connectivity regime regardless of the parameter combinations. Specifically, in order to span the full transition from almost isolated nodes ($\langle k\rangle \to 0$) to almost complete graphs ($\langle k\rangle \gg 1$), we choose five values of the ratio $\langle V(G)\rangle/n$: 0.1, 0.3, 0.5, 0.7 and 0.9; as indicated by the blue horizontal dashed lines in in Figs. 1(c) and 1(d).

As a first example, in Fig. 2 we present the probability distribution function of the normalized number of non isolated vertices $\overline{V}(G)$

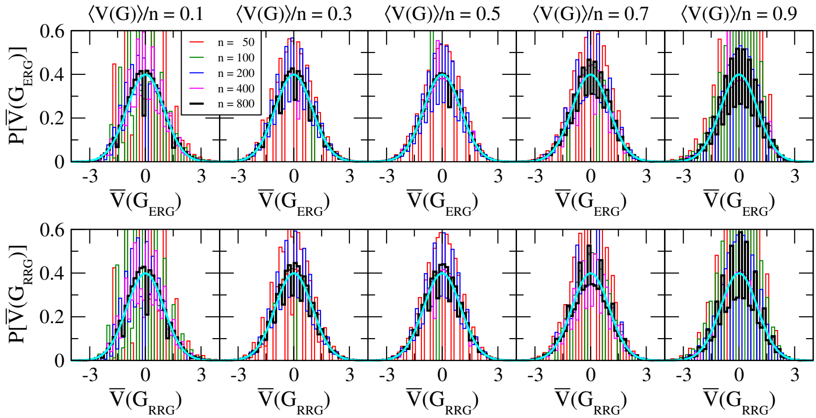

Figure 2. Probability distribution functions of the normalized number non isolated vertices $\overline{V}(G)$ for Erdős-Rényi graphs (upper panels) and for random geometric graphs (lower panels). Each panel displays five histograms corresponding to graphs of different sizes n. Each column corresponds to a fixed value of the ratio $\langle V(G)\rangle/n$. Each histogram is constructed with 10^6 values of $V(G)$. The cyan full line in all panels is a normal distribution with zero mean and unit variance.

$= \langle V(G)\rangle/n$ for both ERGs (upper panels) and RGGs (lower panels) for five values of $\langle V(G)\rangle/n$ (0.1, 0.3, 0.5, 0.7 and 0.9); as indicated on top of the figure. Data were standardized to a zero mean and unit variance. Notice that each panel displays five histograms corresponding to graphs of different sizes n. From this figure we can see, for both random graph models, that the distribution of this degree-based TI converges to a standard normal distribution (represented by the cyan full lines) as the graphs become larger regardless of the value of $\langle V(G)\rangle/n$; see that black histograms in all panels approach the normal distribution.

3 Distribution of topological and spectral indices on Erdős-Rényi graphs

In this section, we analyze the distributions of TIs, MTIs, Revan-degree indices, and spectral indices on ERGs across the full range of connectivity. Results corresponding to RGGs are reported in the Appendix.

3.1 Distribution of degree-based topological indices on Erdős-Rényi graphs

To explore the distribution of TIs, we selected the following well-known indices: The first and second Zagreb indices [15]

$$M_1(G) = \sum_{u \in V(G)} d_u^2 = \sum_{uv \in E(G)} d_u + d_v \tag{8}$$

and

$$M_2(G) = \sum_{uv \in E(G)} d_u d_v, \tag{9}$$

respectively, the Sombor index [14]

$$SO(G) = \sum_{uv \in E(G)} \sqrt{d_u^2 + d_v^2}, \tag{10}$$

the Randić connectivity index [26]

$$R(G) = \sum_{uv \in E(G)} \frac{1}{\sqrt{d_u d_v}}, \tag{11}$$

and the harmonic index [12]

$$H(G) = \sum_{uv \in E(G)} \frac{2}{d_u + d_v}. \tag{12}$$

Based on the results from the previous section, regarding the number of non-isolated vertices $V(G)$, we explore the distribution of TIs in three representative connectivity regimes:

(i) *Sparse regime.* When most vertices are isolated, $\langle V(G) \rangle / n = 0.1$.

(ii) *Intermediate regime.* When the proportion of isolated and non-isolated vertices is approximately equal, $\langle V(G) \rangle / n = 0.5$.

(iii) *Dense regime.* When most vertices are connected, $\langle V(G) \rangle / n = 0.9$.

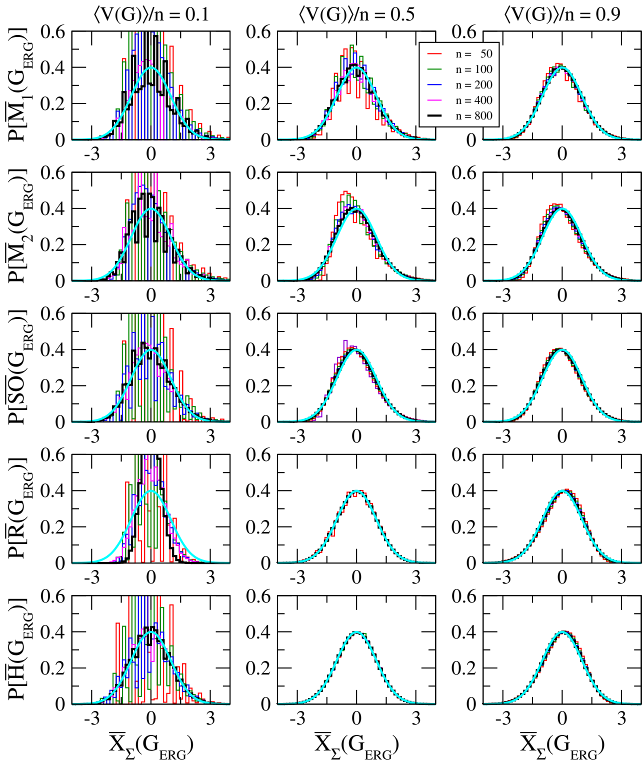

Figure 3. Probability distribution functions of standardized degree-based topological indices on Erdős-Rényi graphs: First Zagreb index $\overline{M}_1(G)$, second Zagreb index $\overline{M}_2(G)$, Sombor index $\overline{SO}(G)$, Randić index $\overline{R}(G)$, and harmonic index $\overline{H}(G)$. Each panel displays five histograms corresponding to graphs of different sizes $n \in [50, 800]$. Each column corresponds to a fixed value of the ratio $\langle V(G)\rangle /n$. Each histogram is constructed with 10^6 values of $X_\Sigma(G)$. The cyan full line in all panels is a normal distribution with zero mean and unit variance.

In Fig. 3 we present the probability distribution functions of the TIs of Eqs. (8)-(12) on ERGs. In this and all the following figures, each panel displays five histograms corresponding to graphs of different sizes $n \in [50, 800]$. Each histogram is constructed from an ensemble of 10^6 random graphs. Also, each column corresponds to a fixed value of the ratio $\langle V(G)\rangle /n$; so, graph connectivity increases from left to right. Moreover, to ease the comparison across regimes and graph sizes, the data is standardized to have zero mean and unit variance:

$$\overline{X}_\Sigma(G) = \frac{X_\Sigma(G) - \mu_{X_\Sigma}}{\sigma_{X_\Sigma}}, \tag{13}$$

where μ_{X_Σ} and σ_{X_Σ} denote, respectively, the mean and standard deviation of the TI $X_\Sigma(G)$.

From this figure, we can clearly observe that the distribution of all the TIs analyzed here tends to a normal distribution (indicated with the cyan line in all panels). It is interesting to note that the normal distribution is approached even in the sparse regime for all TIs (except for the Randić index) when the graph size is large enough; see the black histograms in left panels corresponding to $\langle V(G)\rangle/n = 0.1$. Evidently, for $\langle V(G)\rangle/n = 0.5$ and 0.9 all histograms, even those corresponding to $n = 50$, for all TIs fall on top of the normal distribution. Note that with Fig. 3 we numerically validate the analytical results of Ref. [32] were the distribution of TIs was predicted to converge to a normal distribution.

We now proceed to compute the distributions of MTIs. To this end we consider the following well-known MTIs: The Narumi-Katayama index [24]

$$NK(G) = \prod_{u \in V(G)} d_u, \tag{14}$$

multiplicative versions of the Zagreb indices [31]:

$$\Pi_1(G) = \prod_{u \in V(G)} d_u^2, \tag{15}$$

$$\Pi_2(G) = \prod_{uv \in E(G)} d_u d_v, \tag{16}$$

and

$$\Pi_1^*(G) = \prod_{uv \in E(G)} d_u + d_v, \tag{17}$$

the multiplicative Randić connectivity index [5]

$$R_\Pi(G) = \prod_{uv \in E(G)} \frac{1}{\sqrt{d_u d_v}}, \tag{18}$$

and the multiplicative harmonic index [5]

$$H_{\Pi}(G) = \prod_{uv \in E(G)} \frac{2}{d_u + d_v}. \tag{19}$$

Since the values of MTIs grow exponentially for increasing average degree, see e.g. [5], we compute their logarithms instead. Then, in Fig. 4 we present the probability distribution function of the logarithm of the standardized MTIs of Eqs. (14)-(19) on ERGs. From this figure, we can clearly observe that the distribution of the logarithm all the MTIs analyzed here tends to a normal distribution (indicated with the cyan line in all panels). Remarkably, the normal distribution is approached even in the sparse regime for all MTIs (not shown here) when the graph size is large enough; in fact, $n = 800$ (the larger graph size we used in this work) is not enough to observe the normal distribution in the sparse regime (see the black histograms in left panels corresponding to $\langle V(G) \rangle /n = 0.1$). For $\langle V(G) \rangle /n = 0.5$ and 0.9 all histograms, even those corresponding to $n = 50$, for all MTIs fall on top of the normal distribution.

Therefore, since the distributions of the logarithm of the MTIs follow a normal distribution, we can conclude that the distributions of the MTIs follow a log-normal distribution.

3.2 Distribution of Revan-degree indices on Erdős-Rényi graphs

The Revan-degree indices we choose for our study are: The first and second Revan Zagreb indices [17]

$$R_1(G) = \sum_{u \in V(G)} r_u^2 = \sum_{uv \in E(G)} r_u + r_v \tag{20}$$

and

$$R_2(G) = \sum_{uv \in E(G)} r_u r_v, \tag{21}$$

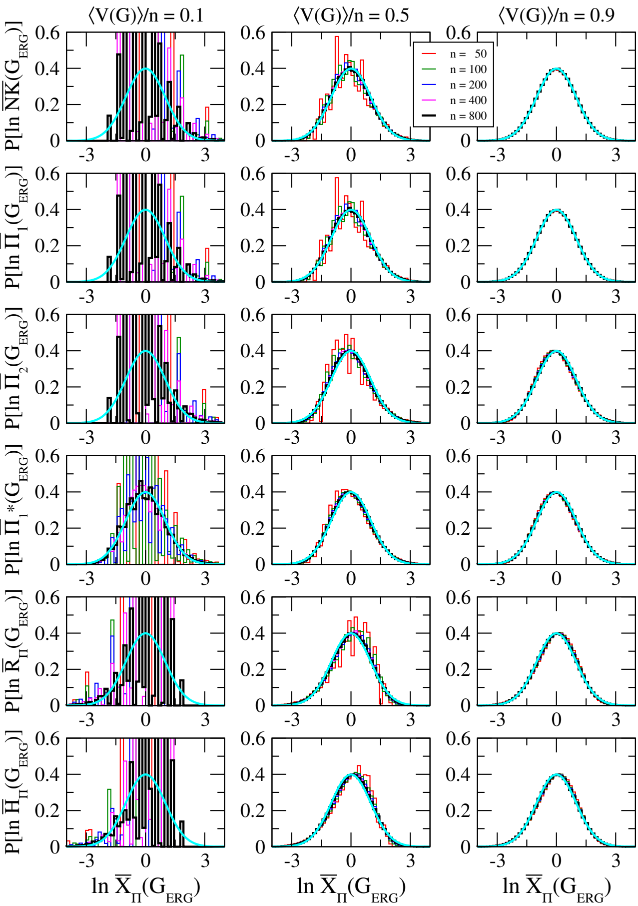

Figure 4. Probability distribution functions of the logarithm of standardized multiplicative topological indices on Erdős-Rényi graphs: Narumi-Katayama index $\overline{NK}(G)$, multiplicative Zagreb indices $\overline{\Pi}_1(G)$, $\overline{\Pi}_2(G)$ and $\overline{\Pi}_1^*(G)$, multiplicative Randić index $\overline{R}_\Pi(G)$, and multiplicative harmonic index $\overline{H}_\Pi(G)$. Each panel displays five histograms corresponding to graphs of different sizes $n \in [50, 800]$. Each column corresponds to a fixed value of the ratio $\langle V(G)\rangle / n$. Each histogram is constructed with 10^6 values of $X_\Pi(G)$. The cyan full line in all panels is a normal distribution with zero mean and unit variance.

respectively, the Revan Sombor index [19]

$$RSO(G) = \sum_{uv \in E(G)} \sqrt{r_u^2 + r_v^2}, \tag{22}$$

the Revan Randić index

$$RR(G) = \sum_{uv \in E(G)} \frac{1}{\sqrt{r_u r_v}}, \tag{23}$$

and the Revan harmonic index

$$RH(G) = \sum_{uv \in E(G)} \frac{2}{r_u + r_v}. \tag{24}$$

We note that, as far as we know, $RR(G)$ and $RH(G)$ are being introduced here.

We also explore the behavior of the distribution of the multiplicative Revan-degree indices, $RX_{\Pi}(G)$: The multiplicative Revan Narumi-Katayama index

$$RNK(G) = \prod_{u \in V(G)} r_u, \tag{25}$$

the multiplicative Revan Zagreb indices

$$R_{1\Pi}(G) = \prod_{u \in V(G)} r_u^2, \tag{26}$$

$$R_{1\Pi^*}(G) = \prod_{uv \in E(G)} r_u + r_v, \tag{27}$$

and

$$R_{2\Pi}(G) = \prod_{uv \in E(G)} r_u r_v, \tag{28}$$

the multiplicative Revan Randić connectivity index

$$RR_{\Pi}(G) = \prod_{uv \in E(G)} \frac{1}{\sqrt{r_u r_v}}, \tag{29}$$

and the multiplicative Revan harmonic index

$$RH_{\Pi}(G) = \prod_{uv \in E(G)} \frac{2}{r_u + r_v}. \tag{30}$$

It is fair to mention that $R_{1\Pi}(G)$ and $R_{2\Pi}(G)$ were introduced in [2]; while, as far as we know, $RNK(G)$, $R_{1\Pi^*}(G)$, $RR_{\Pi}(G)$ and $RH_{\Pi}(G)$ are being introduced here.

In Figs. 5 and 6 we present, respectively, the probability distribution functions of the standardized Revan-degree indices of Eqs. (20)-(24) and the probability distribution functions of the logarithm of the standardized multiplicative Revan-degree indices of Eqs. (25)-(30), both on ERGs. In contrast with TIs and MTIs, see Figs. 3 and 4, we do not observe a clear transition of the distributions of Revan-degree indices nor of the distributions of the logarithm of multiplicative Revan-degree indices to a normal distribution; not even in the dense regime (see the panels in the third columns of Figs. 5 and 6 corresponding to $\langle V(G) \rangle / n = 0.9$). However, in Ref. [2] it was shown that the statistical properties of both Revan-degree indices and multiplicative Revan-degree indices are equivalent to those of their standard-degree counterparts in the dense limit, specifically for $\langle k \rangle > 10$. Thus, we indeed expect to recover normal distributions of both Revan-degree indices the logarithm of multiplicative Revan-degree indices deep enough in the dense limit.

Therefore, we include an additional column in both Figs. 5 and 6 where we set $\langle k \rangle$ to 100; i.e. the graphs are now deeper in the dense regime. So, we can now conclude that, deep in the dense regime, the distributions of Revan-degree indices follow normal distributions while the distributions of multiplicative Revan-degree indices follow log-normal distributions.

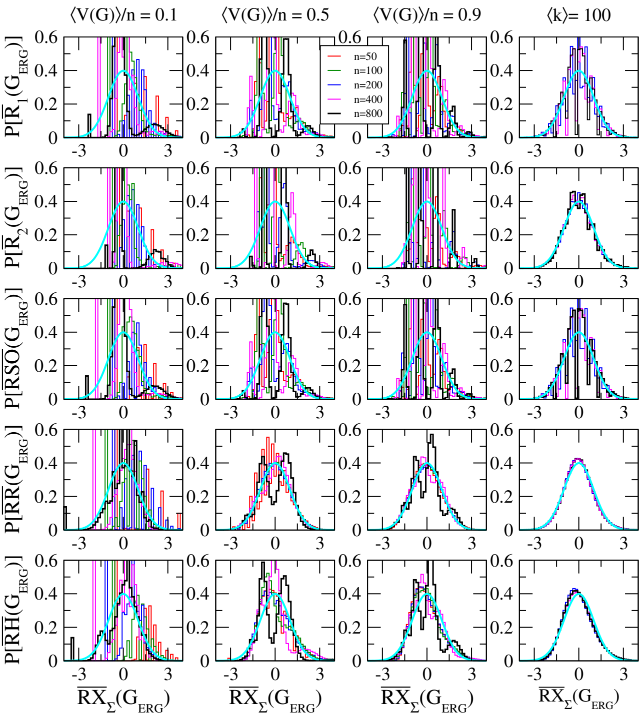

Figure 5. Probability distribution functions of standardized Revan-degree indices on Erdős-Rényi graphs: First Revan Zagreb index $\overline{R}_1(G)$, second Revan Zagreb index $\overline{R}_2(G)$, Revan Sombor index $\overline{RSO}(G)$, Revan Randić index $\overline{RR}(G)$, and Revan harmonic index $\overline{RH}(G)$. Each panel displays five histograms corresponding to graphs of different sizes $n \in [50, 800]$. Each column corresponds to a fixed value of the ratio $\langle V(G)\rangle/n$, except for the right column where $\langle k\rangle = 100$ is set. Each histogram is constructed with 10^6 values of $RX_\Sigma(G)$. The cyan full line in all panels is a normal distribution with zero mean and unit variance.

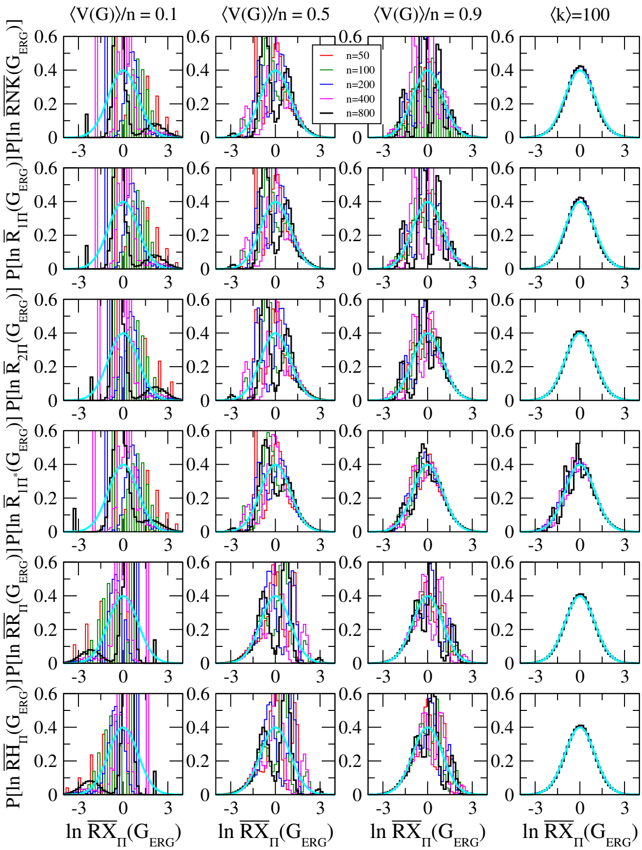

Figure 6. Probability distribution functions of the logarithm of standardized multiplicative Revan-degree indices on Erdős-Rényi graphs: Revan Narumi-Katayama index $\overline{RNK}(G)$, multiplicative Revan Zagreb indices $\overline{R}_{1\Pi}(G)$, $\overline{R}_{2\Pi}(G)$ and $\overline{R}_{1\Pi^*}(G)$, multiplicative Revan Randić index $\overline{RR}_{\Pi}(G)$, and multiplicative Revan harmonic index $\overline{RH}_{\Pi}(G)$. Each panel displays five histograms corresponding to graphs of different sizes $n \in [50, 800]$. Each column corresponds to a fixed value of the ratio $\langle V(G)\rangle /n$, except for the right column where $\langle k\rangle = 100$ is set. Each histogram is constructed with 10^6 values of $RX_{\Pi}(G)$. The cyan full line in all panels is a normal distribution with zero mean and unit variance.

3.3 Distribution of spectral indices on Erdős-Rényi graphs

Finally, we extend our analysis to spectral indices. To this end, we first define a weighted adjacency matrix as follows:

$$A_{ij} = \begin{cases} \sqrt{2}\epsilon_{ii} & \text{for } i = j, \\ \epsilon_{ij} & \text{if there is an edge between vertices } i \text{ and } j, \\ 0 & \text{otherwise.} \end{cases} \tag{31}$$

Here, ϵ_{ij} are statistically independent random variables drawn from a normal distribution with zero mean and unit variance. Once the adjacency matrix is weighted, we diagonalize it and compute the corresponding spectral indices. The spectral indices we consider include Rodríguez-Velázquez indices, the graph energy, and centrality-based indices, which are defined as follows.

Given an orthonormal basis of eigenvectors $\{\Psi_i\}_{i=1}^n$ and the corresponding eigenvalues $\{\lambda_i\}_{i=1}^n$ of the adjacency matrix A of a graph G of size n, the first and second Rodríguez-Velázquez (RV) indices are defined as [28]

$$RV_a(G) = \left(\frac{1}{n} \sum_{i=1}^{n} S_i^2 \right)^{1/2} \tag{32}$$

and

$$RV_b(G) = \sum_{i=1}^{n} x_i S_i, \tag{33}$$

respectively. Here,

$$S_i = \sum_{j=1}^{n} \left(\Psi_j^i \right)^2 \exp(\lambda_j) \tag{34}$$

represents the subgraph centrality while

$$x_i = \frac{1}{\lambda_1} \sum_{j=1}^{n} A_{ij} |\Psi_j^1| \tag{35}$$

denotes the eigenvector centrality of vertex i, where λ_1 is the largest eigenvalue of A and Ψ_j^1 is the jth component of the eigenvector corresponding to λ_1.

Additionally, the graph energy $E(G)$ [16, 21] and the exponential subgraph centrality $EE(G)$ [10] are defined as

$$E(G) = \sum_{i=1}^{n} |\lambda_i|, \tag{36}$$

and

$$EE(G) = \frac{1}{n}\sum_{i=1}^{n} S_i = \frac{1}{n}\sum_{i=1}^{n} \exp(\lambda_i), \tag{37}$$

respectively.

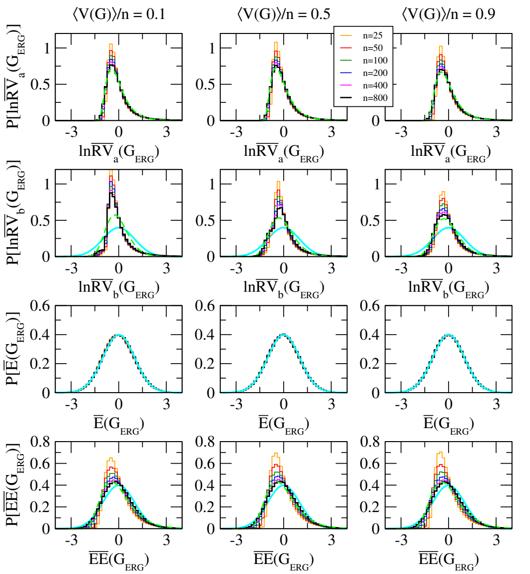

Figure 7. Probability distribution functions of standardized spectral indices on Erdős-Rényi graphs: Rodríguez-Velázquez indices $\overline{RV_a}(G)$ and $\overline{RV_b}(G)$, graph energy $\overline{E}(G)$, and subgraph centrality $\overline{EE}(G)$. Each panel displays six histograms corresponding to graphs of different sizes $n \in [25, 800]$. Each column corresponds to a fixed value of the ratio $\langle V(G)\rangle/n$. Each histogram is constructed with 10^6 values. Magenta full lines are fittings of Eq. (38) to the distributions corresponding to $n = 800$; the values of the fitting parameters are reported in Table 1. The cyan full line in all panels is a normal distribution with zero mean and unit variance.

In Fig. 7 we present the probability distribution functions of standardized spectral indices on ERGs. As well as for MTIs, since RV indices and the exponential subgraph centrality grow exponentially with $\langle k \rangle$, see e.g. [4], we work with the distribution of their logarithms.

From Fig. 7 we can clearly see that, remarkably, the shape of the distributions of spectral indices do not change with the graph connectivity (except for the distribution of $\ln RV_b(G)$ which shows a slight dependence with $\langle V(G) \rangle / n$); this in contrast with the distributions of degree-based indices whose shapes evolve with $\langle V(G) \rangle / n$. We also observe a slight dependence of the distribution shapes with the graph size.

Moreover, note that only the distribution of $E(G)$ exhibits the shape of a normal distribution. In contrast, the distributions of the Rodríguez-Velázquez indices as well as those of $EE(G)$ display an asymmetric, right-skewed, shape. We found that the log-normal distribution function

$$f(x, \sigma, \mu) = \frac{1}{x\sigma\sqrt{2\pi}} \exp\left(-\frac{(\log(x) - \mu)^2}{2\sigma^2}\right) - \beta, \tag{38}$$

fits relatively well the distributions of the Rodríguez-Velázquez indices as well as those of $EE(G)$; see the magenta lines in Fig. 7 which are the fittings of Eq. (38) to the distributions corresponding to $n = 800$. Here, μ and σ are the mean and standard deviation of the spectral indices, in a logarithmic scale, and β is the distribution displacement on the x-axis. The values of the fitting parameters are reported in Table 1.

Index	$\langle V(G) \rangle / n$	σ	μ	β
	0.1	0.4477	0.3206	1.5821
RV_a	0.5	0.4918	0.2336	1.4781
	0.9	0.4307	0.4183	1.7211
	0.1	0.1857	1.3362	3.9269
RV_b	0.5	0.2174	1.2587	3.6506
	0.9	0.2176	1.2814	3.7300
	0.1	0.3252	1.1020	3.1740
EE	0.5	0.3146	1.1243	3.2365
	0.9	0.3095	1.1486	3.3103

Table 1. Values of the parameters σ, μ, and β obtained from the fittings of Eq. (38) to the probability distribution functions (with $n = 800$) of the spectral indices in Fig. 7.

4 Summary

In this work, we performed a thorough statistical (numerical) study of the probability distribution functions of topological and spectral indices on random graphs. Specifically, we computed degree-based topological indices (TIs), degree-based multiplicative indices (MTIs) Revan-degree indices, and spectral indices on two types of random graphs: Erdös-Rényi graphs (ERGs) and random geometric graphs (RGGs).

We performed our study by the use of the following indices.

- TIs: Number of non-isolated vertices, first and second Zagreb indices, Sombor index, Randić index, and harmonic index.
- MTIs: Narumi-Katayama index, multiplicative Zagreb indices, multiplicative Randić index, and multiplicative harmonic index.
- Revan-degree indices: First Revan Zagreb index, second Revan Zagreb index, Revan Sombor index, Revan Randić index, and Revan harmonic index. Also, Revan Narumi-Katayama index, multiplicative Revan Zagreb indices, multiplicative Revan Randić index, and multiplicative Revan harmonic index.
- Spectral indice: Rodríguez-Velázquez indices, graph energy, and subgraph centrality.

It is relevant to mention that previos studies of the distributions of TIs were reported in Refs. [22, 23, 33, 34]. However, the statistical studies of Refs. [22, 23] were not exhaustive while the analytical studies of Refs. [33, 34] were not numerically verified, so in this work we believe we fill those gaps. Therefore, our results can be summarized as follows.

For both ERGs and RGGs:

(i) asymptotically, for large enough connectivity and graph size, the distributions of the TIs follow a normal distribution (see Figs. 3 and 8);

(ii) asymptotically, for large enough connectivity and graph size, since the distributions of the logarithm of the MTIs follow a normal distribution (see Figs. 4 and 9), the distributions of the MTIs follow a log-normal distribution;

(iii) deep in the dense limit, the distributions of the Revan-degree indices follow a normal distribution (see Figs. 5 and 10);

(iv) deep in the dense limit, since the distributions of the logarithm of the multiplicative Revan-degree indices follow a normal distribution (see Figs. 6 and 11), the distributions of the multiplicative Revan-degree indices follow a log-normal distribution;

(v) the distribution of the graph energy exhibits the shape of a normal distribution for any graph connectivity and graph size (see Figs. 7 and 12);

(vi) the distributions of the Rodríguez-Velázquez indices as well as those of the subgraph centrality follow an asymmetric, right-skewed, log-normal distribution (see Eq. (38) and Figs. 7 and 12).

We finally stress that our results validate the analytical prediction of Ref. [32] stating that the distributions of TIs on ERGs converge to normal distributions; see Fig. 3. However, and even more interesting, our results contradict the prediction of Ref. [34] which claims that the limiting distribution of the Randić index on RGGs is not the standard normal distribution; see Fig. 8.

We hope our results may motivate further analytical studies.

***Acknowledgment*:** J.A.M.-B. thanks support from VIEP-BUAP (Grant No. 100405811-VIEP2025), Mexico. C.T.M.-M. Thanks for the support from CONAHCYT (CVU No. 784756).

References

[1] R. Aguilar-Sanchez, I. F. Herrera-Gonzalez, J. A. Mendez-Bermudez, J. M. Sigarreta, Computational properties of general indices on random graphs, *Symmetry* **12** (2020) #1341.

[2] R. Aguilar-Sanchez, I. F. Herrera-Gonzalez, J. A. Mendez-Bermudez, J. M. Sigarreta, Revan-degree indices on random graphs, preprint arXiv:2210.04749, **doi:** `https://doi.org/10.48550/arXiv.2210.04749`.

[3] R. Aguilar-Sanchez, J. A. Mendez-Bermudez, F. A. Rodrigues, J. M. Sigarreta-Almira, Topological versus spectral properties of random geometric graphs, *Phys. Rev. E* **102** (2020) #042306.

[4] R. Aguilar-Sanchez, J. A. Mendez-Bermudez, J. M. Rodriguez, J. M. Sigarreta, Analytical and statistical studies of Rodriguez-Velazquez indices, *J. Math. Chem.* **59** (2021) 1246–1259.

[5] R. Aguilar-Sanchez, J. A. Méndez-Bermúdez, J. M. Rodriguez, J. M. Sigarreta, Multiplicative topological indices: Analytical properties and application to random graphs, *AIMS Math.* **9** (2024) #3646.

[6] V. Consonni, R. Todeschini, New spectral indices for molecule description, *MATCH Commun. Math. Comput. Chem.* **60** (2008) 3–14.

[7] J. Dall, M. Christensen, Random geometric graphs, *Phys. Rev. E* **66** (2002) #016121.

[8] P. Erdös, A. Rényi, On random graphs, *Publ. Math. (Debrecen)* **6** (1959) 290–297.

[9] P. Erdös, A. Rényi, On the evolution of random graphs, Inst. Hung. Acad. Sci. **5** (1960) 17–61; P. Erdös, A. Rényi, On the strength of connectedness of a random graph, *Acta Math. Hungar.* **12** (1961) 261–267.

[10] E. Estrada, J. A. Rodriguez-Velazquez, Subgraph centrality in complex networks, *Phys. Rev. E* **71** (2005) #056103.

[11] E. Estrada, M. Sheerin, Random rectangular graphs, *Phys. Rev. E* **91** (2015) #042805.

[12] S. Fajtlowicz, On conjectures of Graffiti–II, *Congr. Numer.* **60** (1987) 187–197.

[13] I. Gutman, Degree-based topological indices, *Croat. Chem. Acta* **86** (2013) 351–361.

[14] I. Gutman, Geometric approach to degree–based topological indices: Sombor indices, *MATCH Commun. Math. Comput. Chem.* **86** (2021) 11–16.

[15] I. Gutman, N. Trinajstić, Graph theory and molecular orbitals. Total π-electron energy of alternant hydrocarbons, *Chem. Phys. Lett.* **17** (1972) 535–538.

[16] I. Gutman, H. Ramane, Research on graph energies in 2019, *MATCH Commun. Math. Comput. Chem.* **84** (2020) 277–292.

[17] V. R. Kulli, Revan indices of oxide and honeycomb graphs, *Int. J. Math. Appl.* **5** (2017) 663–667.

[18] V. R. Kulli, F-Revan index and F-Revan polynomial of some families of benzenoid systems, *J. Global Res. Math. Archives* **5** (2018) 1–6.

[19] V. R. Kulli, I. Gutman, Revan Sombor index, *J. Math. Inform.* **22** (2022) 23–27.

[20] V. R. Kulli, J. A. Méndez-Bermúdez, J. M. Rodriguez, J. M. Sigarreta, Revan Sombor indices: Analytical and statistical study, *Math. Biosci. Eng.* **20** (2023) 1801–1819.

[21] X. Li, Y. Shi, I. Gutman, *Graph Energy*, Springer, Berlin, 2012.

[22] C. T. Martínez-Martínez, J. A. Mendez-Berḿudez, J. M. Rodríguez, J. M. Sigarreta, Computational and analytical studies of the Randić index in Erdös–Rényi models, *Appl. Math. Comput.* **377** (2020) #125137.

[23] C. T. Martínez-Martínez, J. A. Mendez-Bermudez, J. M. Rodríguez, J. M. Sigarreta, Computational and analytical studies of the harmonic index in Erdös–Rényi models, *MATCH Commun. Math. Comput. Chem.* **85** (2021) 395–426.

[24] H. Narumi, M. Katayama, Simple topological index – A newly devised index characterizing the topological nature of structural isomers of saturated hydrocarbons, *Mem. Fac. Eng. Hokkaido Univ.* **16** (1984) 209–214.

[25] M. Penrose, *Random Geometric Graphs*, Oxford University Press, Oxford, 2003.

[26] M. Randić, On characterization of molecular branching, *J. Am. Chem. Soc.* **97** (1975) 6609–6615.

[27] M. Randić, On characterization of chemical structure, *J. Chem. Inf. Comput. Sci.* **37** (1997) 672–687.

[28] J. A. Rodriguez-Velazquez, A. T. Balaban, Two new topological indices based on graph adjacency matrix eigenvalues and eigenvectors, *J. Math. Chem.* **57** (2019) 1053–1074.

[29] R. Solomonoff, A. Rapoport, Connectivity of random nets, *Bull. Math. Biophys.* **13** (1951) 107–117.

[30] N. Trinajstić, *Chemical Graph Theory*, CRC Press, 2018.

[31] R. Todeschini, V. Consonni, New local vertex invariants and molecular descriptors based on functions of the vertex degrees, *MATCH Commun. Math. Comput. Chem.* **64** (2010) 359–372.

[32] M. Yuan, On the Randić index and its variants of network data, *TEST* **33** (2023) 155–179.

[33] M. Yuan, Asymptotic distribution of degree-based topological indices, *MATCH Commun. Math. Comput. Chem.* **91** (2025) 135–196.

[34] M. Yuan, Limiting distribution for the Randić index of a random geometric graph, *MATCH Commun. Math. Comput. Chem.* **93** (2024) 767–789.

[35] M. Yuan, X. Zhao, Asymptotic distributions of the average clustering coefficient and its variant, preprint arXiv:2311.10979, **doi:** `https://doi.org/10.48550/arXiv.2311.10979`.

Appendix: Distribution of topological and spectral indices on random geometric graphs

In this Appendix, we report our results on the distributions of topological and spectral indices on RGGs, see Figs. 8–12. Note that Figs. 8–12 for RGGs are equivalent to Figs. 3–7 for ERGs, respectively. Indeed, from Figs. 8–12 we draw similar conclusions as those already discussed in the main text for ERGs:

(i) Asymptotically, for large enough connectivity and graph size, the distributions of the TIs follow a normal distribution; see Fig. 8.

(ii) Asymptotically, for large enough connectivity and graph size, since the distributions of the logarithm of the MTIs follow a normal distribution (see Fig. 9), the distributions of the MTIs follow a log-normal distribution.

(iii) Deep in the dense limit, the distributions of the Revan-degree indices follow a normal distribution; see Fig. 10.

(iv) Deep in the dense limit, since the distributions of the logarithm of the multiplicative Revan-degree indices follow a normal distribution (see Fig. 11), the distributions of the multiplicative Revan-degree indices follow a log-normal distribution.

(v) The distribution of the graph energy exhibits the shape of a normal distribution for any graph connectivity and graph size; see Fig. 12.

(vi) The distributions of the Rodríguez-Velázquez indices as well as those of the subgraph centrality follow an asymmetric, right-skewed, log-normal distribution; see Fig. 12 and Eq. (38).

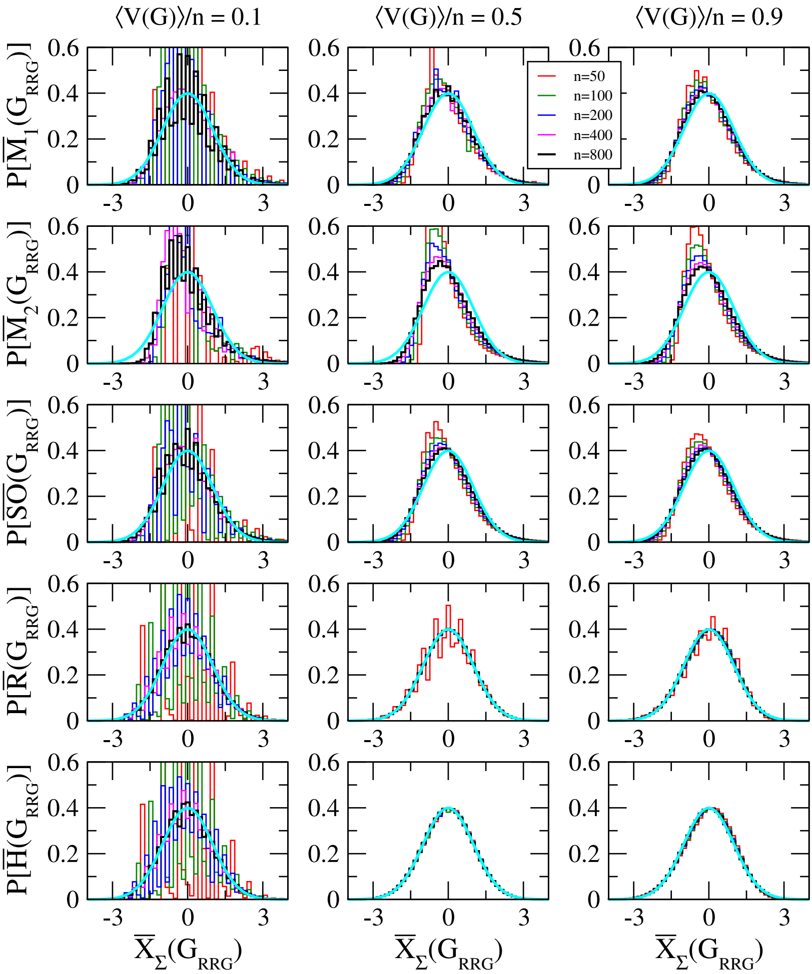

Figure 8. Probability distribution functions of standardized degree-based topological indices on random geometric graphs: First Zagreb index $\overline{M}_1(G)$, second Zagreb index $\overline{M}_2(G)$, Sombor index $\overline{SO}(G)$, Randić index $\overline{R}(G)$, and harmonic index $\overline{H}(G)$. Each panel displays five histograms corresponding to graphs of different sizes $n \in [50, 800]$. Each column corresponds to a fixed value of the ratio $\langle V(G) \rangle / n$. Each histogram is constructed with 10^6 values of $X_\Sigma(G)$. The cyan full line in all panels is a normal distribution with zero mean and unit variance.

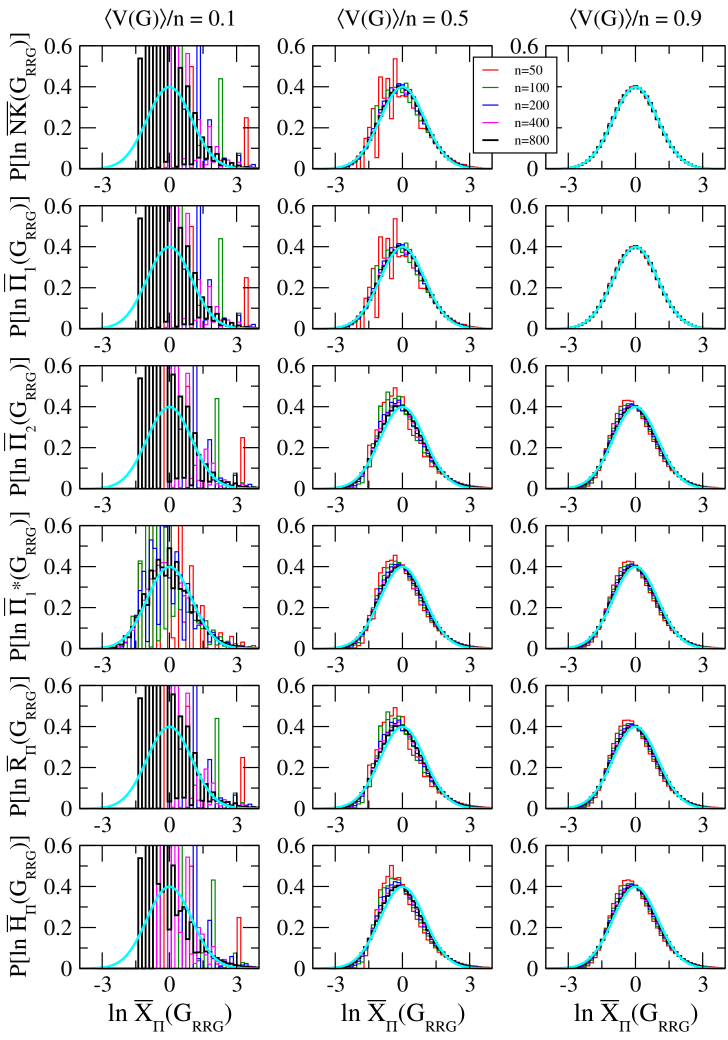

Figure 9. Probability distribution functions of the logarithm of standardized multiplicative topological indices on random geometric graphs: Narumi-Katayama index $\overline{NK}(G)$, multiplicative Zagreb indices $\overline{\Pi}_1(G)$, $\overline{\Pi}_2(G)$ and $\overline{\Pi}_1^*(G)$, multiplicative Randić index $\overline{R}_\Pi(G)$, and multiplicative harmonic index $\overline{H}_\Pi(G)$. Each panel displays five histograms corresponding to graphs of different sizes n, ($n \in [50, 800]$). Each column corresponds to a fixed value of the ratio $\langle V(G)\rangle / n$. Each histogram is constructed with 10^6 values of $X_\Pi(G)$. The cyan full line in all panels is a normal distribution with zero mean and unit variance.

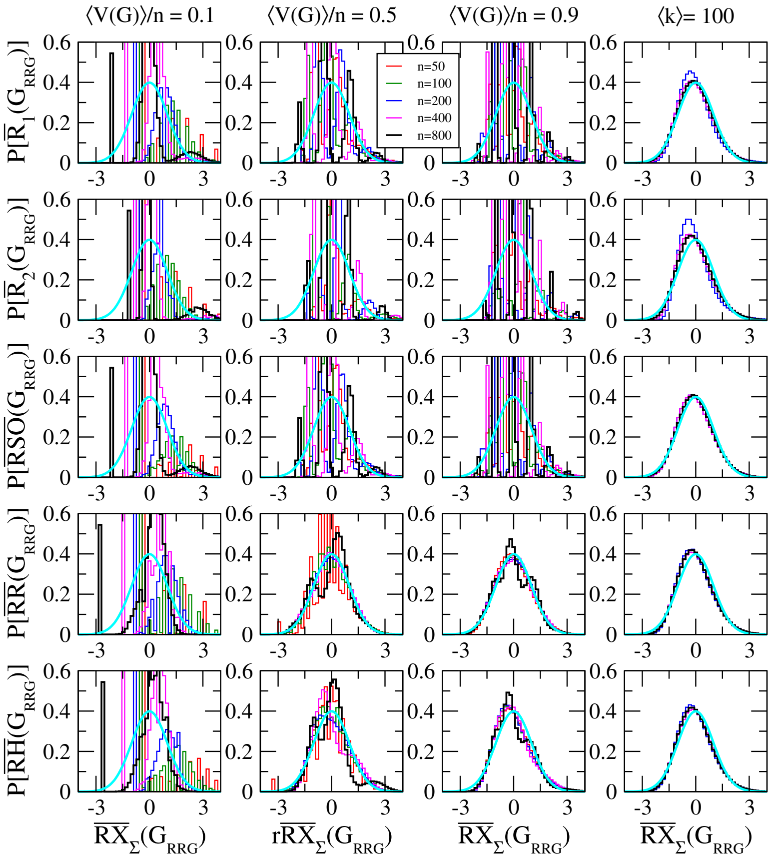

Figure 10. Probability distribution functions of standardized Revan-degree indices on random geometric graphs: first Revan Zagreb index $\overline{R}_1(G)$, second Revan Zagreb index $\overline{R}_2(G)$, Revan Sombor index $\overline{RSO}(G)$, Revan Randić index $\overline{RR}(G)$, and Revan harmonic index $\overline{RH}(G)$. Each panel displays five histograms corresponding to graphs of different sizes $n \in [50, 800]$. Each column corresponds to a fixed value of the ratio $\langle V(G)\rangle / n$, except for the right column where $\langle k \rangle = 100$ is set. Each histogram is constructed with 10^6 values of $RX_\Sigma(G)$. The cyan full line in all panels is a normal distribution with zero mean and unit variance.

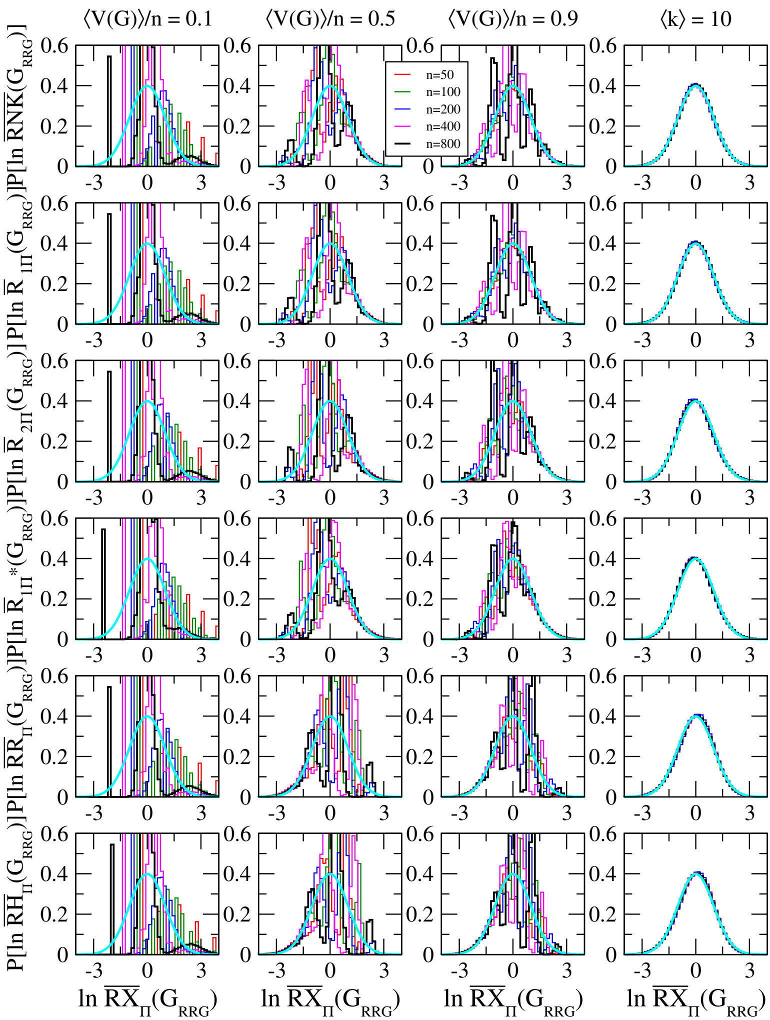

Figure 11. Probability distribution functions of the logarithm of standardized multiplicative Revan-degree indices on random geometric graphs: Revan Narumi-Katayama index $\overline{RNK}(G)$, multiplicative Revan Zagreb indices $\overline{R}_{1\Pi}(G)$, $\overline{R}_{2\Pi}(G)$ and $\overline{R}_{1\Pi^*}(G)$, multiplicative Revan Randić index $\overline{RR}_\Pi(G)$, and multiplicative Revan harmonic index $\overline{RH}_\Pi(G)$. Each panel displays five histograms corresponding to graphs of different sizes $n \in [50, 800]$. Each column corresponds to a fixed value of the ratio $\langle V(G)\rangle/n$, except for the right column where $\langle k\rangle = 10$ is set. Each histogram is constructed with 10^6 values of $RX_\Pi(G)$. The cyan full line in all panels is a normal distribution with zero mean and unit variance.

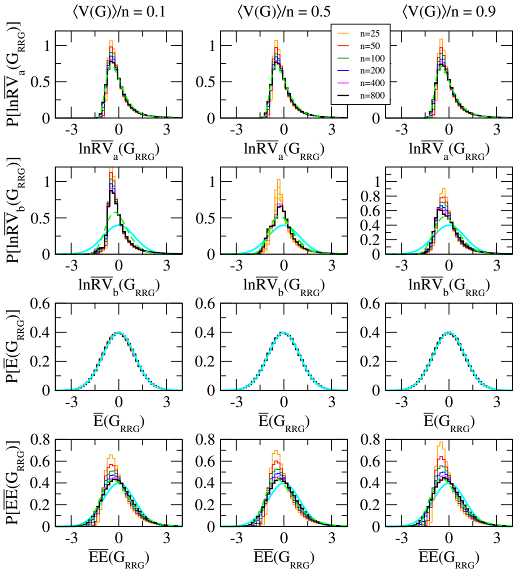

Figure 12. Probability distribution functions of standardized spectral indices on random geometric graphs: Rodríguez-Velázquez indices $\overline{RV_a}(G)$ and $\overline{RV_b}(G)$, graph energy $\overline{E}(G)$, and subgraph centrality $\overline{EE}(G)$. Each panel displays six histograms corresponding to graphs of different sizes $n \in [25, 800]$. Each column corresponds to a fixed value of the ratio $\langle V(G)\rangle /n$. Each histogram is constructed with 10^6 values. Magenta full lines are fittings of Eq. (38) to the distributions corresponding to $n = 800$; the values of the fitting parameters are reported in Table 2. The cyan full line in all panels is a normal distribution with zero mean and unit variance.

Index	$\langle V(G)\rangle /n$	σ	μ	β
RV_a	0.1	0.4613	0.2753	1.5226
	0.5	0.4763	0.2569	1.5029
	0.9	0.4901	0.2581	1.5114
RV_b	0.1	0.1838	1.3414	3.9450
	0.5	0.2067	1.3149	3.8484
	0.9	0.2032	1.3552	3.9998
EE	0.1	0.2682	1.2775	3.7256
	0.5	0.3186	1.1073	3.1873
	0.9	0.3374	1.0406	3.0007

Table 2. Values of the parameters σ, μ, and β obtained from the fittings of Eq. (38) to the probability distribution functions (with $n = 800$) of the spectral indices in Fig. 12.